RESEARCH ARTICLE

INTERNATIONAL RESEARCH JOURNAL OF MULTIDISCIPLINARY TECHNOVATION

Asian Research Association

DOI:10.54392/irjmt26219

Cuttlefish Bone as a Natural Source of Hydroxyapatite: Characterization and Cell Line Analysis

A. Nirmala [a], R. Devika [a,*]

[a] Department of Biotechnology, Aarupadai Veedu Institute of Technology, Vinayaka Missions Research Foundation (DU), Paiyanoor - 603 104, Chengalpattu district, Tamil Nadu, India

* Corresponding Author Email: devika@avit.ac.in

DOI: https://doi.org/10.54392/irjmt26219

Received: 23-09-2025; Revised: 04-03-2026; Accepted: 19-03-2026; Published: 30-03-2026

Abstract: Biomaterials are man-made substances used to replace the damaged tissues in the body to restore the normal function. In recent years there has been growing interest in developing biomaterials from natural sources such as shells, fish scales, bones, plants, and algae for bone and dental applications. Cuttlefish bones, rich in calcium carbonate and easily available as marine waste, eco-friendly, non-toxic, low cost for calcium carbonate production and suitable for biomedical usage. In present study waste cuttlefish bone collected, cleaned, washed and dried were ground into fine powder. This powder was calcined through a thermal process to produce calcium oxide, from which hydroxyapatite (HAp) was isolated. The synthesized HAp was characterized using FTIR spectroscopy (analyzing raw bones, Calcium oxide and HAp), SEM with EDX, TEM, X-ray diffraction (XRD), and tested for antimicrobial activity against pathogens including Gram-positive bacteria (*Streptococcus mutans, Bacillus subtilis*) and Gram-negative bacteria (*Alcaligenes faecalis, Pseudomonas aeruginosa*). Cell viability assays were performed using MG63 osteoblastcells with the synthesized HAp nanoparticles. From the study we observed that the FTIR analysis shows the presence of calcium carbonate in raw cuttlefish bones, while calcium oxide showed characteristic peaks for C-H bending, C-N stretching, S=O stretching, C=O stretching, and O-H stretching. SEM images revealed quasi-spherical, nanoscale particles with significant agglomeration and EDX confirmed the presence of calcium, phosphorus, oxygen, and carbon as primary components. TEM validated the nanoscale size of particles. Antimicrobial testing showed higher HAp concentrations (750 and 1000 µg/ml) effectively inhibited both Gram (+) ve and Gram (-) ve bacteria. Additionally, HAp demonstrated over 50% cell viability with MG63 cells, indicating good biocompatibility. Cuttlefish bone derived HAp shows significant as biocompatible, antimicrobial properties with potent biomaterial for biomedical use.

Keywords: Biomaterial, HAp, Biocompatibility, Osteoconductive, Anti-Microbial Activity

1. Introduction

The field of nanotechnology and nano drugs have led to numerous discoveries with notable advancements in nano medicine significantly impacting healthcare. Continued research is essential to fully realize the potential of nanotechnology in healthcare. In medicine, extensive studies are being conducted on optimal methods for treating conditions such as nephrology, cardiovascular diseases and cancer. Traditional treatments have seen remarkable progress, while the development, refinement of nanotechnology and nanoparticles have yielded promising results [1]. In medical field the nanoparticles have been applied in gene therapy, numerous studies focusing on the use of viral vectors as drug delivery systems [2-4]. Carbohydrates, Proteins, lipids and other organic molecules can produce the nanoparticle, which are usually characterized by a radius of less than 100 nm. In comparison, inorganic nanoparticles are recognized for their nontoxic nature, hydrophilicity, biocompatibility, and superior stability compared to their organic counterparts.

The sources or wastes of natural hydroxyapatite includes mammalian bones (examples such as clam, eggshell, cockle and seashell), shells (examples like clam, cockle, seashell and eggshell), marine or aquatic sources (examples like animal bone and fish scale) plants, algae and mineral sources (example-limestone). In comparison to other mammalian sources such as camel, horse and porcine the extraction of hydroxyapatite (HAp) from bovine bone is often documented. [5-7]. The cortical region of the femur is most commonly utilized due to its structural and physical similarity to human bone. The Ca/P ratio, size, structure and crystaline phases of calcium phosphate are the various characteristics of the extracted HAp that have

been discussed in many literature reviews. These properties can differ based on the extraction methods employed, as well as factors such as pH and calcination temperatures [8]. Many chemical precursors can be used to synthesis the hydroxyapatite in a number of ways, such as wet and dry processes, thermal treatments and combinations of these techniques [9]. The techniques employed in the synthesis influence the size, chemical composition, crystallinity, and morphology of the resulting hydroxyapatite, which in turn affect its mechanical strength, biological properties, biocompatibility and bioactivity.

Cuttlefish shells (CS) represent an inexpensive and readily available resource, but their disposal can lead to contamination of air, water and soil. The demand for the natural resource particularly cuttlefish bone expected to increase as the world population predicted to reach 9.8 billion by 2050 [10]. Additionally, it is anticipated that approximately two-thirds of the world's inhabitants will live in urban areas, consuming about 75% of the planet's natural resources and producing half of its waste [11]. To effectively address this waste challenge, implementing circular economy (CE) principles—focusing on reduction, reuse, and recycling—is essential [12,13].

The cuttlefish bone, known as "Samudraphena," is derived from a specific type of fish with 10 arms, a round body and an unattractive appearance. It has intimidating eyes and a hard back similar to that of a tortoise. After animal dies, all its organs disintegrate and the cuttlefish bone floats on the sea's surface like foam, eventually collecting on the shore. This is commonly known as cuttlefish bone [14]. Its size varies from approximately 3 inches to around 6 feet and its body is adorned with brown cross bands and purple spots, exhibiting a metallic sheen in sunlight and displaying the ability to change color. The cuttlefish utilizes its arms to both cling to objects and capture marine life for sustenance. Additionally, it possesses an internal shell known as the cuttlefish bone, which is broad, spongy and chalky [15]. The aragonite form of calcium carbonate ($CaCO_3$) and trace minerals including sodium, magnesium and strontium which importantly contribute to the bone healing process [16, 17]. Nonetheless, the analysis of this waste has been methodically performed to evaluate its suitability for various biomedical applications.

2. Materials and Methods

2.1. Collection of Sample and Preparation

The cuttlefish bone was purchased from a commercial pet shop (Figure.1a). The dorsal shield, which is the thick outer layer of the bone, was carefully removed with a lancet (Figure.1b). After taking the inner part, it was thoroughly cleaned with tap water and washed with distilled water twice afterwards dried in a hot air oven 3 to 4 hours at 80 °C. A mortar and pestle were used to grind the dried cuttlefish bone in to fine powder, stored in sterile container and kept in desiccator at room temperature to prevent contamination (Figure.1c).

2.2. Synthesis of Calcium Oxide

The dried cuttlefish bone powder 10 gm was subjected to heating in a muffle furnace at 450°C for 2 hours to remove impurities after that it was calcinated at 900°C for 3 hours. During this process carbon dioxide released as a byproduct which transformed the calcium carbonate into calcium oxide. The validation of the synthesized calcium carbonate was carried out through various test (solubility test, Reaction with water, litmus paper test, Sodium hydroxide test and Ammonia test). The calcium oxide was then sieved to achieve uniform particle size and stored for subsequent applications.

2.3. HAp Synthesis from Cuttlefish Bone

The process used to synthesize the HAp was modified from the technique used by Adeogun *et al.,*2017; Kamalanathan *et al.*, 2014; Ćurković *et al.,* 2017 [18-20]. Dissolved 1 M of calcined cuttlefish bone powder in 50 mL of distilled water after that 0.6 M of phosphoric acid (H_3PO_4) gradually added until pH reached 8.5 (Figure-2a).

Fig-1a Fig-1b Fig-1c

Figure1a. Collection of Cuttle fish bone, **b.** Dorsal side removed cuttle bone, **c.** Cuttle bone powder

(a) (b)

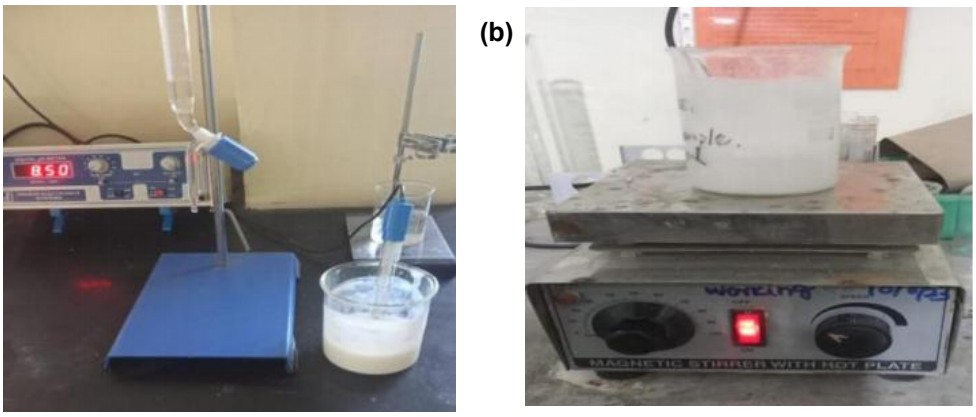

Figure 2a. PH adjusted to reach 8.5, **b.** Sample stirred in Magnatic stirrer

To facilitate the precipitation, the mixture was kept at room temperature for 24 hours.To guarantee the complete precipitation, it was stirred once again for 30minutes (Figure -2b) with a magnetic stirrer (100 rpm) and left for another 24 hours without any disturbance. After that, the resulting solution was filtered and washed with distilled water for 2 hours and it was dried at 100°C. The dried precipitate was subsequently calcined at 900°C temperatures in a furnace for 2 hours. The synthesized hydroxyapatite was stored in a clean container for further analysis.

2.4 Characterization Studies

2.4.1. Fourier Transform Infrared (FTIR) Spectroscopy

The functional groups present in the sample was analyzed by using FTIR spectroscopy. The infrared spectra, covering a wave-number range of 400 to 4000 cm^{-1}, were obtained using a Perkin Elmer Spectrum instrument (version 10.02.00) with translucent pellets. These pellets were prepared by blending the powdered samples with potassium bromide (KBr). The measurements involved four scans conducted at a resolution of 2 cm^{-1}.

2.4.2. Scanning Electron Microscopy (SEM) and Energy Dispersion Spectroscopy (EDS)

Using HITACHI S5500 microscope made for non-conductive materials and running at an accelerating voltage of 3–5 kV, the morphology and aggregation condition of the hydroxyapatite (HAp) samples were examined.Droplet evaporation was used to prepare the sample: A small amount of sample approximately 1-5µg/mL was dissolved in ethanol, which was placed on the SEM stage until the ethanol completely get evaporated [21, 22]. The maximum Feret diameter (MF) of the HAp NOAA was determined from over 1500 particles across images magnified at 400×. The Image J software was used to automatically execute these analyses on representative SEM images. SEM combined with an X-ray microanalyzer (EDS, energy dispersive spectroscopy) were used for the initial chemical analysis. The EDS measurements were conducted in dark-field mode at an accelerating voltage of 8 kV, with a 2-minute scan duration, accumulating approximately 10,000 counts. Quantitative analysis involved examining at least 15 different agglomerates per sample. The data were collected using a High-Resolution Scanning Electron Microscope, EVO 10 model, equipped with the Smart EDX EDS system from Carl Zeiss, Germany, featuring a LaB6 (Lanthanum hexaboride) filament as the electron source.

2.4.3. Transmission Electron Microscopy (TEM)

The HAp sample was sonicated for 20 minutes at a concentration of 75 µg/mL according to standard protocols before TEM analysis. TEM images with Image J software (National Institutes of Health, Bethesda, MD, USA) were used to measure the particle size. A Gaussian (normal distribution) curve was plotted using GraphPad Prism version 8 (GraphPad Software, San Diego, CA, USA) to evaluate the size distribution of the particle.

2.4.4. X-Ray Diffraction (XRD)

Crystallographic structure of the HAp sample was analyzed using X-ray diffraction (XRD) method. Using the established protocols, the measurements were carried out at a scan rate of 0.02° per minute within a 2θ range of 20° to 80°.

2.4.5. Antimicrobial Activity Studies with Isolated HAp

During the period of study two Gram negative organisms (*Alcaligenes faecalis, Pseudomonas aeruginosa)* and Gram positive organisms (*Streptococcus mutans* and *Bacillus subtilis)* were inoculated in the nutrient broth for anti-microbial studies with isolated HAp at different concentrations (1000, 750, 500, 250 and 100 mg/ml) in the respective wells. Ciprofloxacin, used as a positive control, was applied at a concentration of 10 µg/mL, while DMSO served as the

negative control. A bacterial suspension containing 10^6 CFU/mL of each tested strain was spread onto nutrient agar plates. Until the turbidity matched with 5 McFarland standard the broth culture was incubated at 37°C. After the incubation time, the sterile distilled water was used to modify the bacterial culture until its turbidity matched with standard.

2.4.6. Cell Cytotoxicity Assay

The cell cytotoxicity assay was carried out by using (3- (4, 5-dimethyl thiazol-2yl) - 2, 5- diphenyl tetrazolium bromide (MTT) [23]. In 96 well plate the cells were trypsinized and incubated at 37°C for 24 hours. After incubation, various concentrations of MG63 cells were exposed to samples for a period of 12 to 24 hours. The MTT experiment was carried out by adding MTT, which is converted in to purple formazan product by mitochondrial succinate dehydrogenase and reductase in the living cell. The amount of formazan formed was measured spectrophotometrically, which correlates with the number of viable cells and decreases with increasing cytotoxicity. After treatment, the media were aspirated from the wells, which were then incubated for 4 hours at room temperature with MTT solution (5 mg/ml prepared in phosphate-buffered saline). A microplate reader was used to detect the absorbance at 570nm after the formazan crystals were dissolved in 100 µl of DMSO. Also, to achieve appropriate concentration, about 1 mg of each sample was mixed with sterile complete medium and diluted properly.

3. Result and Discussion

3.1. Confirmatory Tests for Calcium Oxide

The synthesized calcium oxide was confirmed with various solubility tests with water, ethanol, ammonia and glycerol the observed results are illustrated in the Table -1.

Organic and moisture content decompose rapidly when exposed to temperatures exceeding 500°C, resulting in noticeable changes in the samples' appearance. Since bones are primarily composed of $CaCO_3$, they undergo significant structural and chemical transformations during this process. The powder samples illustrated the different colour changes that occur due to calcination process at various temperature levels as shown in the figure. 3a to 3c.

The cuttlefish bone initially exhibits a light-yellow color (original state) (Figure-3a). When the sample was heated at 450°C in a muffle furnace(Figure-3b), it turned to a brownish-black shade, whereas at 900°C, the powder appears significantly whiter (Figure-3c). During the calcination process the moisture loss and release of carbon dioxide is responsible for the color changes. According to Suwannasingha *et al.* [24], 900°C is considered the ideal temperature for the breakdown of $CaCO_3$. Achieving high temperatures is essential for the effective conversion of cuttlefish bone into CaO. The darker coloration observed at lower temperatures suggests incomplete decomposition of the bone powder.

3.2 HAp Synthesis from Calcium Oxide Isolated from Cuttlefish Bone

The synthesized calcium oxide was exposed to phosphoric acid precipitation which resulted in white precipitate of HAp. The synthesized HAp crystals were stored in clean container for further characterization studies.

3.3 Characterization Studies of HAp from Cuttle Fish Bone

3.3.1 Fourier Transform Infrared Spectroscopy analysis (FTIR)

3.3.1.1 FTIR Analysis of Raw Cuttle Fish Bone Powder

Raw cuttle fish bone powder was subjected to FTIR analysis and the functional groups are illustrated in Table -2 and the FTIR Peaks are represented in Fig-4. The FTIR spectral bands of raw cuttlebone were recorded at 542, 711, 852, 1080, 1440, 1651, 1794, 2362, 2525, 3373 and 3746. Based on the peak values the following functional compounds were identified in cuttlefish bone powder indicated the presence of the existence of aragonite carbonates or presence of calcium carbonate.

Table 1. Confirmatory test results of calcium oxide

S.no	Confirmative tests	Observation
1	Solubility in water	Slight solubility in water
	Solubility in Ethanol	Insoluble in ethanol
	Solubility in Glycerol	Insoluble in glycerol
2	Reaction with water	Heatgeneration was observed
3	Litmus paper test	Red litmus paper turns to blue
4	Sodium hydroxide test	White precipitate was formed
5	Ammonia test	Faint-white precipitate observed

Fig-3a Fig-3b Fig-3c

Figure 3a. Cuttle bone powder, **b.** Cuttlebone powder at 450°C, **c** at900°C powder appears white

Table 2. Functional groups identified in raw cuttlefish bone powder

S.no	Peak value	Functional group	Class
1	542	C-Br stretching	halo compound
2	711	C=C bending	alkene
3	852	C-Cl stretching	halo compound
4	1080	C-O stretching	primary alcohol
5	1440	O-H bending	carboxylic acid
6	1651	C-H bending	aromatic compound
7	1794	C-H bending	aromatic compound
8	2362	O=C=O stretching	carbon dioxide
9	2525	O-H stretching	Carboxylic acid
10	3373	N-H stretching	aliphatic primary amine
11	3746	O-H stretching	alcohol

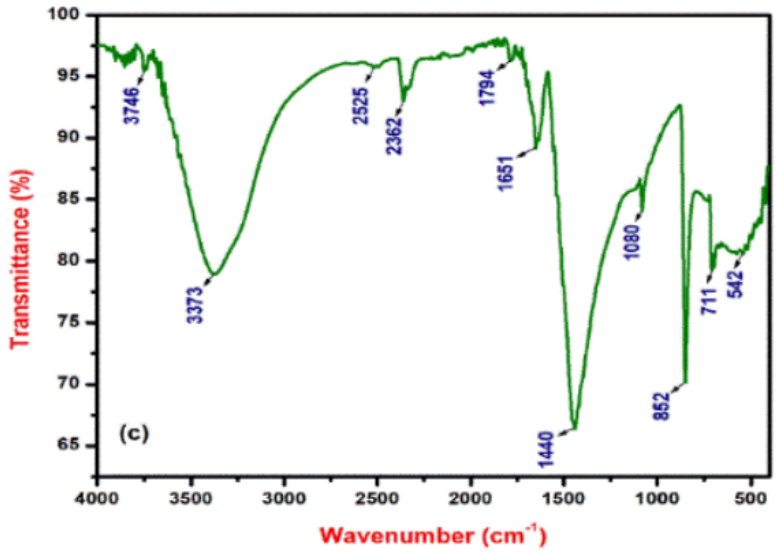

Figure 4. FTIR spectrum of raw cuttle fish bone powder

The standard reference showed the spectrum at 876 and 712 cm^{-1} for compounds containing calcite ($CaCO_3$).

3.3.1.2 FTIR analysis of synthesized calcium oxide from cuttle fish bone

The synthesised CaO from cuttle fish bone powder registered C=C bending, C-H bending, C-N streching, S=O streching, C=O streching and O-H stretching when subjected to FTIR analysis which corresponds to alkene, 1, 2, 4 trisubstituted, amine, sulfate, conjugated acid halide and alchol, respectively (Table-3 and Figure-5). It was observed that O-H stretching appeared may be related to partial surface hydration after calcination (due to the presence of moisture). The presence of CaO was confirmed in both standard reference [25] and sample at 872cm^{-1}

Table 3. Functional groups identified in calcium oxide powder by FTIR analysis

S.no	Peak value	Functional group	Class
1	713	C=C bending	alkene
2	872	C-H bending	1,2 4, trisubstituted
3	1122	C-N stretching	amine
4	1413	S=O stretching	sulfate
5	1794	C=O stretching	conjugated acid halide
6	3646	O-H stretching	Alchol

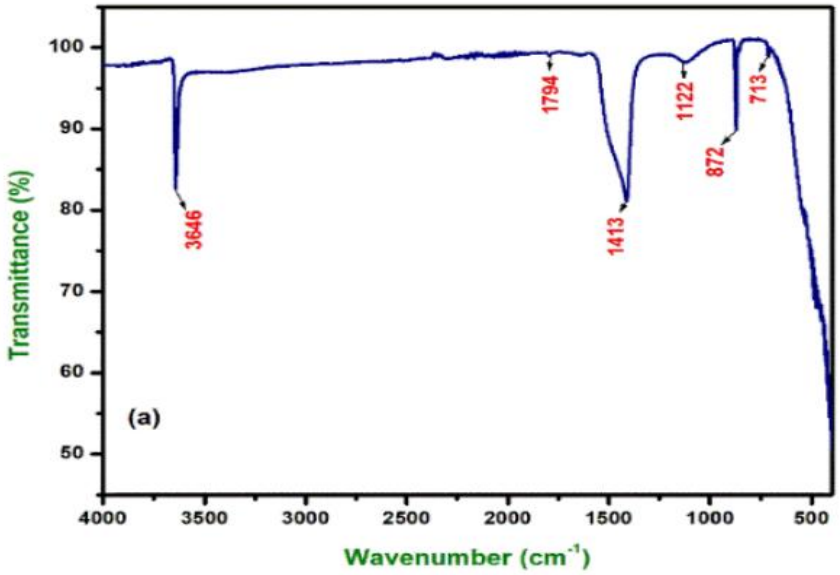

Figure 5. FTIR spectrum of Calcium oxide synthesized from cuttle fish bone

3.3.1.3 FTIR Analysis of Synthesized HAp from Calcium Oxide Isolated from Cuttle Fish Bone

Around 8 peaks namely C-Cl stretching at 561 and 601, C-H bending at 877cm^{-1}, C=C bending at 963cm^{-1}, C-N stretching at 1022cm^{-1}, O-H bending at 1415cm^{-1}, C-H bending at 1453cm^{-1}, C=N stretching at 1694cm^{-1}, representing the halo compound, 1, 2,4 trisubstituted, alkene, amine, carboxylic acid, alkane and imine / oxime respectively. According to the previous study the FTIR spectrum of HAp powder showed sharp bands PO_4^{-3} at 1025-1029 cm^{-1} and spectral peaks from HA Sigma Aldrich were observed at 559.36 cm^{-1}, 601.79 cm^{-1}, 964.41 cm^{-1}, 1022, 27 cm^{-1} respectively.(Table- 4 and Figure-6).

Based on the FTIR peak values, the following functional compounds were identified in cuttle fish bone indicated the presence of the existence of aragonite carbonates or presence of calcium carbonate. The standard reference showed the spectrum at 876 and 712 cm^{-1} for compounds containing calcite ($CaCO_3$). A similar kind of study was conducted by Skandalis *et al.*, [2017] [22] and observed FTIR peaks at 698.23, 713.66, 852.54, 1080.14, 1446.61, and 1786.08 cm^{-1}. According to the study by Mossman [26] the FTIR spectral band peaks were recorded at 710, 860, 1486, 2522, and 2924 cm^{-1} which indicated the existence of aragonite carbonates. Synthesized Calcium oxide spectrum was observed that O-H stretching appeared may be related to partial surface hydration after calcination. The presence of CaO was confirmed in both standard reference [25] and sample at 872cm^{-1}. FTIR spectrum of HAp powder synthesized from calcium oxide showed sharp bands PO_4^{-3} at 1025-1029 cm^{-1} and spectral peaks from HA Sigma Aldrich. Our present study in accordance to Cozza *et al.*, they reported that the sharpen peaks of PO_4^{-3} (peak at 1000cm^{-1}) implies that the crystallinity of the hydroxyapatite powder was good [27].

3.3.2 Scanning Electron Microscopy (SEM) and Energy Dispersion Spectroscopy (EDS)

The surface morphology characterization of the synthesized HAp was analysed using Scanning Electron Microscopy (SEM) (Figure-7a, & b). The morphology of the synthesized HAp powder recorded quasi-spherical and strongly agglomerated due to their small particle size in the nanometer range, with nanometric sizes exhibit better bioactive property.

Table 4. Functional groups identified in synthesized HAp particle

S.no	Peak value	Functional group	Class
1	561	C-Cl stretching	Halo compound
2	601	C-Cl stretching	Halo compound
3	877	C-H bending	1,2,4-trisubstituted
4	963	C= C bending	alkene
5	1022	C-N stretching	amine
6	1415	O-H bending	carboxylic acid
7	1453	C-H bending	alkane
8	1649	C=N stretching	Imine /oxime

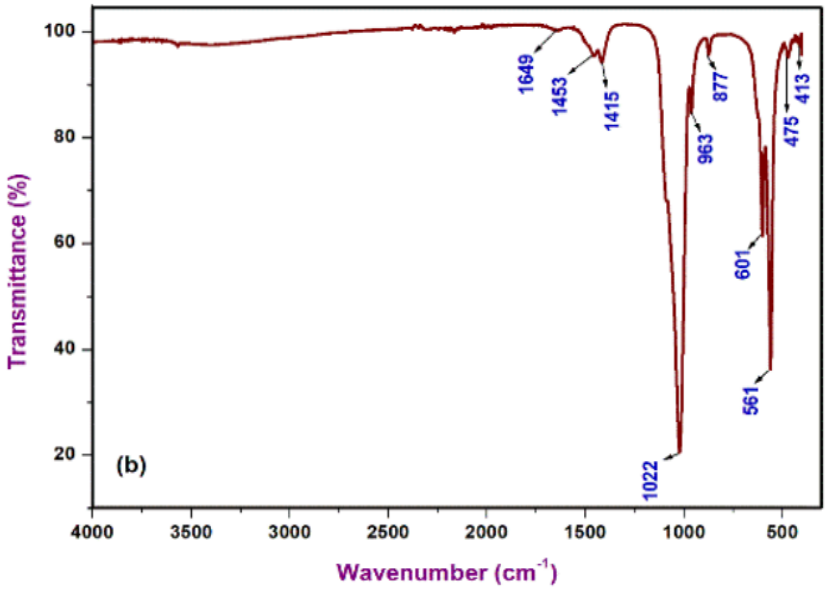

Figure 6.FTIR spectrum of HAP synthesized from Calcium oxide

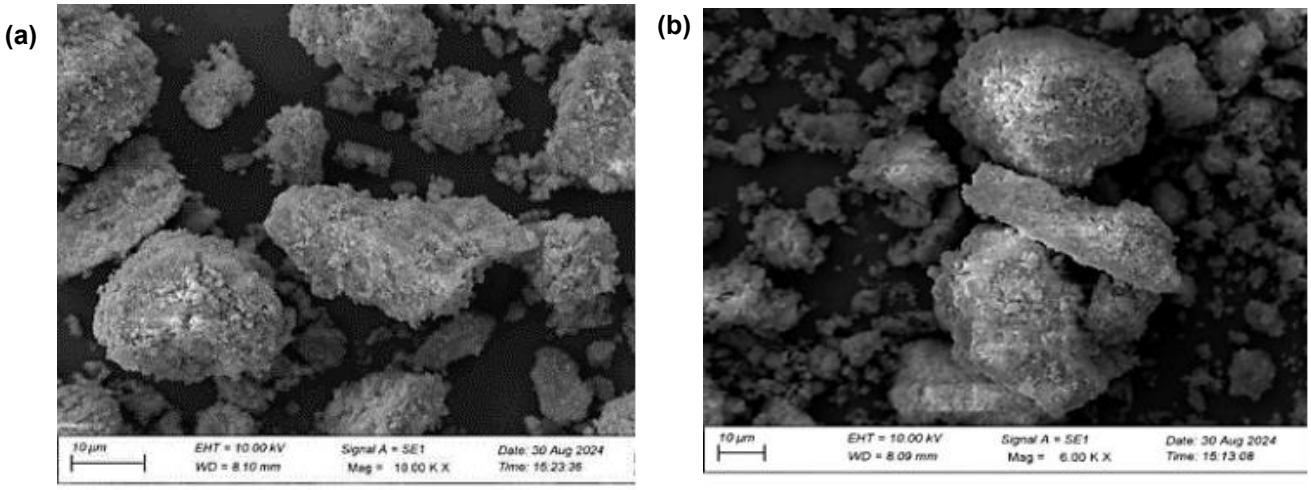

Figure 7a). SEM results of HAp at 600x**, b)** SEM results of HAp at 1000x

The synthesised HAp EDAX analyses revealed and confirmed that inorganic phases of cuttlefish bones were mainly composed of calcium, phosphorus, oxygen and carbon (Figure 8a, b). From the present data the elemental composition of the calcined powder registered major sharp peaks in the spectrum like calcium, phosphours, oxygen and carbon, respectively. The study result finds that, calcined cuttlefish bone HAp particle was the source of stoichiometric HAp made of calcium and phosphorus with a Ca/P mole ratio of 1.67.

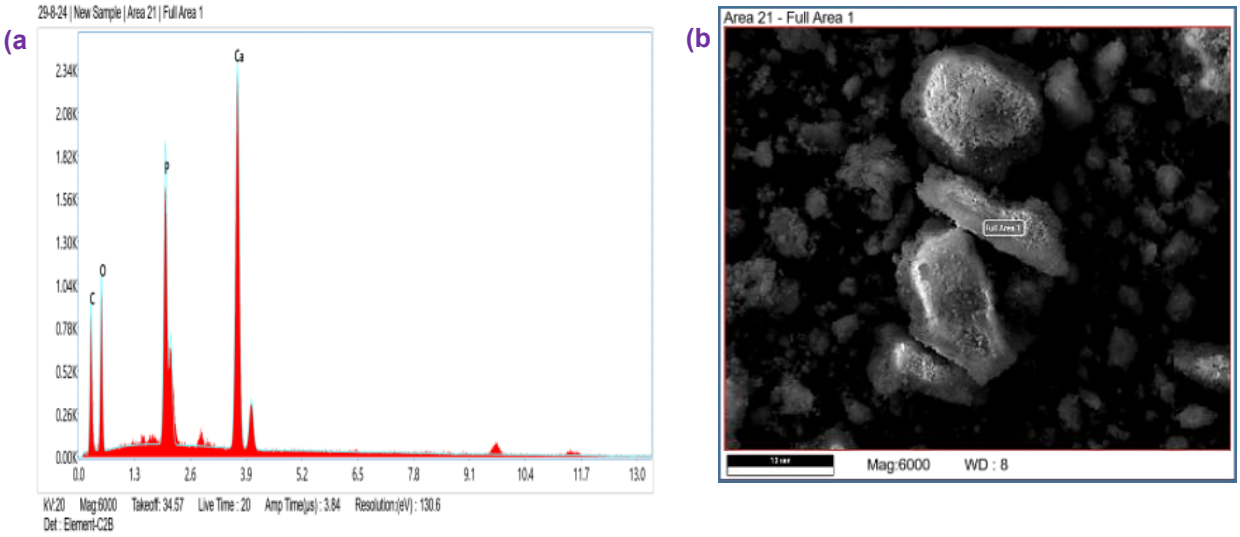

Figure 8 a) EDAX spectrum of synthesised HAp **b)** EDAX analysis of HAp particle.

The SEM analysis of HAp observed single particle characteristics tend to form spherical shape indicating that the particles formed are of nano size which is suitable for application in the field of dentistry [28].The present study results are consistent with previously reported studies which stated that HAp crystals tend to agglomerate [29]. Synthesised HAp EDAX analyses elemental composition of the calcined powder registered major sharp peaks in the spectrum like calcium, phosphours, oxygen and carbon, respectively. The similar result was observed by Stanciu *et al.*[30] their study results revealed the elemental composition of the calcined powders with major sharp peaks at 43.29 wt. % calcium, 39.36 wt. % oxygen, and 16.31 wt. % P, while minor peaks of magnesium and aluminum were identified in trace amounts at 0.57 wt. % and 0.46 wt. %, respectively. EDS analysis of the extracted HAp from fish bone and the percentage atomic ratios of the Ca/P of extracted HAp from fish bone were 1.82, and 1.68, respectively which was higher than those of the stoichiometric HAp.

3.3.3 Transmission Electron Microscopy (TEM)

TEM analysis of HAp revealed the existence of spherical and rod shaped morphology which exhibited particle sizes approximately 16.9nm, 92.1nm 128nm and 129nm, respectively (Figure 9 a to 9d)

TEM analysis of HAp revealed the existence of spherical and rod shaped (40 and 60 nm) morphology from snail shells reported by Parajuli *et al.,* [31]. The stochastic variables in the size and morphology are attributed due to different in heating rates and synthesis periods which eventually influences their biological characteristics [32].

3.3.4 XRD analysis of synthesized HAp

XRD analysis of isolated HAp during the period of study exhibited a single hexagonal crystal structure (Figure 10) which was compared and confirmed with the standard HAp (Joint Committee on Powder Diffraction Standards). Crystalline structure of synthesized HAp particle showed intense peaks (2θ values) at 26.44°, 29.52°, 32.26°, 33.29°, 34.49°, 40.31°, 47.16° and 50.07° with prominent peaks such as002, 211,300, 202 and 213.

XRD analysis of isolated HAp during the period of study exhibited a single hexagonal crystal structure which was in accordance with previous researches [33, 34]. Thus, it is apparent that the chemical change at pH 8.54 expedited the conversion of calcium oxide in to HAp particle and on prolonged heating of calcite crystal revealed relaxation of the lattice of calcite to assist the formation of HAp [35].

3.3.5 Anti-microbial activity studies with isolated HAp

Antibacterial activity studies were carried with synthesized HApon Gram positive organisms (*Streptococcus mutans* and *Bacillus subtilis*) and Gram negative organisms (*Alcaligenes faecalis, Pseudomonas aeruginosa*) in duplicate during the period of studies. The antimicrobial activities of HAp against selected microorgansims after 24 hrs cultures is presented as MIC values in Table-5 and Fig-11. A control test (negative (DMSO) and positive (Ciprofloxacin) was also performed to determine their effect on the specified microorganisms. From the study observed that at higher concentration of HAp (1000 µg/ml and 750 µg/ml) showed a stronger antibacterial activity against the selected Gram positive (*Streptococcus mutans* and *Bacillus subtilis*) and Gram negative organisms (*Alcaligenes faecalis, Pseudomonas aeruginosa)*. At less concentration (500 µg/ml) *Alcaligenes faecalis and Pseudomonas aeruginosa* (Gram negative organism) did not show any significant antimircobial activity against HAp.

There is no zone of inhibition noticed at 250µg/ml against the selected microorganism (both Gram postive and negative).

From the study observed that at higher concentration of HAp (1000 µg/ml and 750 µg/ml) showed in figure 11 a stronger antibacterial activity against the selected Gram positive (*Streptococcus mutans* and *Bacillus subtilis*) and Gram negative organisms (*Alcaligenes faecalis, Pseudomonas aeruginosa)*. This may be due to gram negative bacteria have thicker cell wall and negatively charged peptidoglycan while positively charged HAp particles did not exhibit any significant antimicrobial activity at a lower concentration [36]. Similar outcome was also reported by Jensen *et al.,* [37] where the antibacterial activity was observed only at higher concentrations of nano-HAp, specifically at 50 mg/ml and no activity below 30 mg/ml.

3.3.6 Cell Cytotoxicity Assay

In biomedical field the hydroxyapatite (HAp) is a commonly used bio ceramic material due to its similarity to the mineral component of bone and teeth. It exhibits biocompatibility and bioactivity allowing surrounding tissues to integrate with the implant. Additionally, its porous structure enhances tissue bonding for improved implant stability. To enhance the bio-compatibility the utilization of HAp in the medical field is normally as a coating for metal-based implant [22]. Cytotoxicity testing of any material is the preliminary test to determine the biocompatibility of implant materials. The MTT assay is commonly used method for cytotoxicity testing, providing a quantitative evaluation of cytotoxicity levels *in vitro*. The human osteobalstic cell line MG63 was used in the current research to investigate the cytotoxicity of HAp particle at diverse concentration (1, 2, 4, 8, 16, 32, 64, 128, 256, and 512 µ /ml (Table -6) and sample alone without HAp served as control.

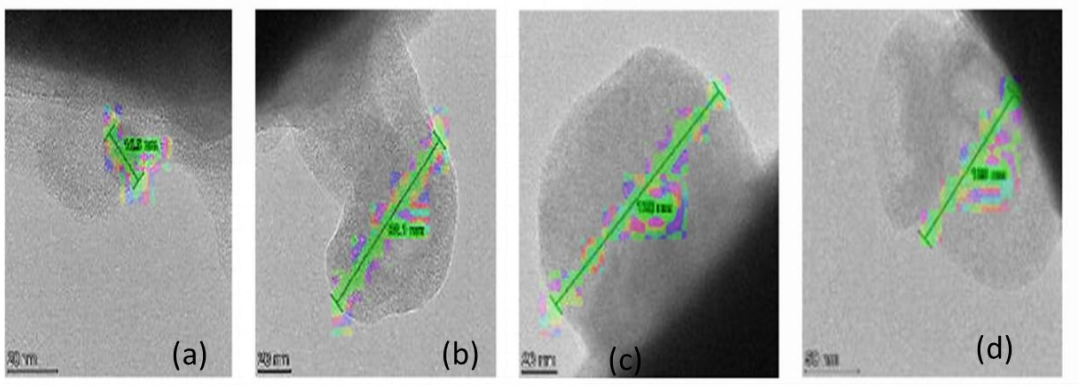

Figure 9a-d. TEM images of HAp at different Nanometer ranges

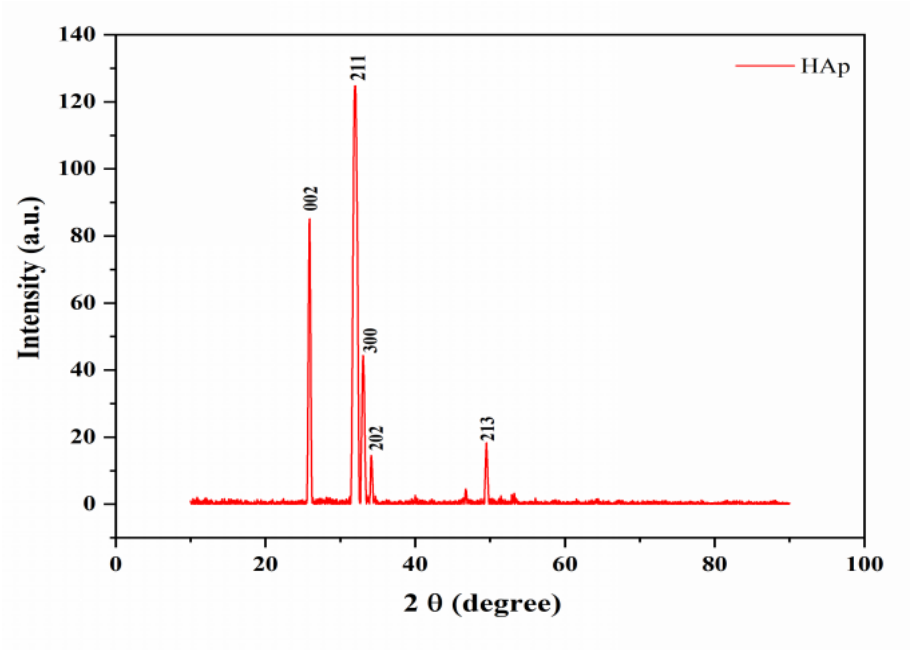

Figure 10. XRD analysis of synthesized HAp particle

Table 5. Antibacterial activity studies with synthesized HAp

Zone ofinhibition (mm)				
HAp concentration (µg/ml)	***Alcaligenes faecalis***	***Pseudomonas aeruginosa***	***Streptococcus mutans***	***Bacillus subtilis***
1000	19	17	21	19
750	16	15	18	16
500	-	-	15	14
250	-	-	-	-
100	-	-	-	-
PC	25	23	26	26
NC	-	-	-	-

*PC – Positive control, NC – Negative control

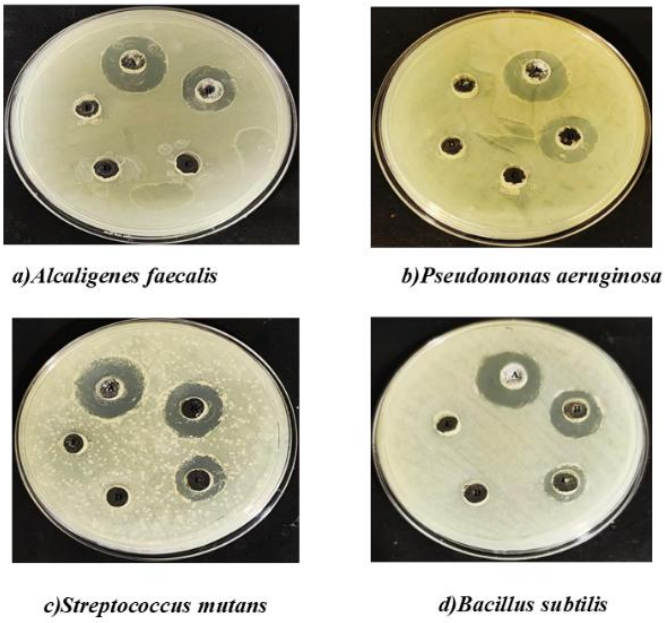

Figure 11. Zone of inhibition of HAp particle against gram (+) &(-)organism

Table 6. Cell cytotoxicity study of HAp particle against MG 63 cell line

Concentration (µg/ml)	% Viability	% Viability	% Viability	Average % Viability	Standard Deviation
512	30.249	31.898	31.093	31.080	31.080 ± 0.824
256	35.745	35.837	35.477	35.686	35.686 ± 0.187
128	44.048	44.147	44.192	44.129	44.129 ± 0.073
64	54.406	55.113	55.329	54.949	54.949 ± 0.482
32	63.325	62.958	63.390	63.224	63.224 ± 0.232
16	70.863	69.619	70.143	70.208	70.208± 0.624
8	79.676	79.735	79.624	79.678	79.678±0.055
4	83.465	83.249	83.203	83.306	83.306±0.139
2	86.043	86.763	86.940	86.915	86.915±0.957
1	95.046	94.896	95.256	95.066	95.066±0.180

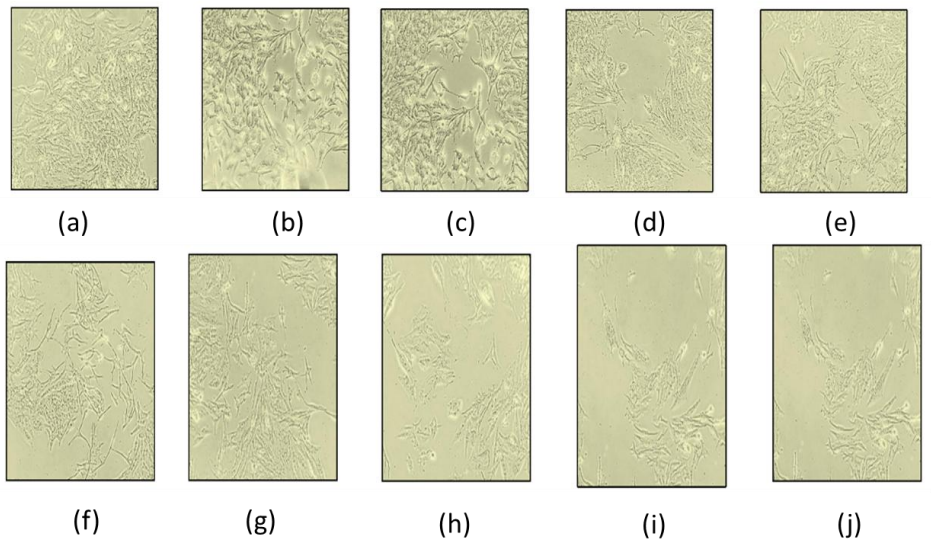

Figure 12 a to j. Cytotoxicity assay of HAp particle against MG63 cell line

All the sample concentration was prepared in triplicates. The respective cytotoxicity assay of HAp particles against MG63 cell line is shown in figure 12 a-j. 1µ/ml to 64 µ/ml HAp particle concentration registered more than 50% cell viability. The average percentage of viability (54.949%) was observed at HAp concentration 64µ/ml.The ISO 2017 standard states that a material is considered to be nontoxic it the cell viability greater than 60%.

During the period of study with cell line MG 36 more than 60 % cell viability was observed at concentration of HAp 32µ/ml. The results of the MTT test demonstrated proved that the synthesized hydroxyapatite from cuttle fish bone is biocompatible and non-toxic and will be an efficient proved bone graft material on further biological investigations [33,34].

4. Conclusion

Based on the present study results it has been concluded that hydrothermal process was most suitable for the synthesis of hydroxyapatite from natural sources (cuttlefish bone waste) and calcinated HAp was found to be superior with specific functional groups, structure etc. Hydroxyapatite isolated from cuttle fish bone showed similarity in morphology, composition and non-toxicity revealed in the literature and may be suitable as a substitution in dental, medical drugs etc. in near future. Although the results obtained so far are promising, further clinical trials with a larger number of samples are needed to better clarify the biological effects of systems containing hydroxyapatite nanoparticles.

References

[1] K. Vishwakarma, O.P. Vishwakarma, M.A. Bhatele, (2012) Brief Review on the Role of Nanotechnology in Medical Sciences. Proceedings of All India Seminar on Biomedical Engineering. (AISOBE 2012). Lecture Notes in Bioengineeing, Springer, India. https://doi.org/10.1007/978-81-322-0970-6_7

[2] K.H. Keskinbora, M.A. Jameel, Nanotechnology applications and approaches in medicine: a review. Journal of Nanoscience and Nanotechnology, 2(2), (2018) 6-8.

[3] S. Quader, X. Liu, K. Toh, Supramolecular Enabled Ph-Triggered Drug Action at Tumor Microenvironment Potentiates Nanomedicine Efficacy Against Glioblastoma. Bio-Materials, 267, (2021) 120463.

[4] M. Azimzadeh, M. Rahaie, N. Nasirizadeh, M. Daneshpour, H. Naderi-Manesh. Electrochemical Mirna Biosensors: the Benefits of Nanotechnology. Nanomedical Research Journal, 1(3), (2017) 158-171.

[5] R. Bayford, T. Rademacher, I. Roitt, S.X. Wang, Emerging applications of nanotechnology for diagnosisand therapy of disease: a review. Physiology Measurement, 38(8), (2017) R183. https://doi.org/10.1088/1361-6579/aa7182

[6] K. Alorku, M. Manoj, A.A. Yuan, Plant-mediated synthesis of nanostructured hydroxyapatite for biomedical applications: a review. RSC Advances, 10, (2020) 40923–40939. https://doi.org/10.1039/D0RA08529D

[7] V. Kalaiselvi, R. Mathammal, S. Vijayakumar, Microwave assisted Green Synthesis of Hydroxyapatite Nanorods using Moringa Oleifera Flower Extract and its Antimicrobial Applications. International Journal of Vetinary Sciences Medicine, 6(2), (2018) 286–295. https://doi.org/10.1016/j.ijvsm.2018.08.003

[8] M.K. Herliansyah, D.A. Nasution, M. Hamdi, A. Ide-Ektessabi, M.W. Wildan, A.E. Tontowi, Preparation and Characterization of Natural Hydroxyapatite: a Comparative Study of Bovine Bone Hydroxyapatite and Hydroxyapatite from Calcite, Material Science Forum, 561–565, (2007)1441–1444. https://doi.org/10.4028/www.scientific.net/MSF.561-565.1441

[9] D.S. Gomes, A.M.C. Santos, G.A. Neves, R.R. Menezes, A Brief Review on Hydroxyapatite Production and Use in Biomedicine. Ceramica, 65,(2019)282–302. http://dx.doi.org/10.1590/036669132019653742706

[10] F. Haque, C. Fan, Y.Y. Lee, From Waste to Value: Addressing the Relevance of Waste Recovery to Agricultural Sector in Line With Circular Economy. Journal of Cleaner Production, 415, (2023) 137873. https://doi.org/10.1016/j.jclepro.2023.137873

[11] T. Maddalene, K. Youngblood, A. Abas, K. Browder, E. Cecchini, S. Finder, S. Gaidhani, W. Handayani, N.X. Hoang, K. Jaiswal, E. Martin, S. Menon, Q. O'Brien, P. Roy, B. Septiarani, N.H. Trung, C. Voltme, M. Werner, R. Wong, J.R. Jambeck, Circularity in cities: A Comparative tool to Inform Prevention of Plastic Pollution. Resources, Conservation and Recycling, 198, (2023) 107156. https://doi.org/10.1016/j.resconrec.2023.107156

[12] R. Cooney, D.B. de Sousa, A. Fernández-Ríos, S. Mellett, N. Rowan, A.P. Morse, M. Hayes, J. Laso, L. Regueiro, A.H. Wan, E.A. Clifford, Circular Economy framework for Seafood Waste Valorisation to Meet Challenges and Opportunities for Intensive Production and Sustainability. Journal of Cleaner Production, 392, (2023) 136283. https://doi.org/10.1016/j.jclepro.2023.136283

[13] N. Yadav, R. Kumar, Performance and Economic Analysis of the Utilization of Construction and Demolition Waste as Recycled Concrete Aggregates. International Journal of Engineering, 37(3), (2024) 460–467. https://doi.org/10.5829/ije.2024.37.03c.02

[14] Sharma Sri Sadananda, Rasatarangini, 11 editions, New Delhi: 11thedition, Motilal Banarasidas. (2004), 306-307, 12/124- 126.

[15] V. Dole, A. Paranjpe, A text book of Rasashastra, Varanasi, chaukhambha, (2019), 17, 386.

[16] D. Reinares-Fisac, S. Veintemillas-Verdaguer, L. Fernández-Díaz, Crystalline Engineering Communication, 19, (2017), 110–116.https://doi.org/10.1039/C6CE01725H

[17] J. Venkatesan, P.D. Rekha, S. Anil, I. Bhatnagar, P.N. Sudha, C. Dechsakulwatana, S.K. Kim, M.S. Shim. Hydroxyapatite from Cuttlefish Bone: Isolation, Characterizations, and applications. Biotechnology and Bioprocess Engineering, *23*(4), (2018) 383-393. https://doi.org/10.1007/s12257-018-0169-9

[18] A.I. Adeogun, A.E. Ofudje, M.A. Idowu, S.O. Kareem, Facile Development of Nano Size Calcium Hydroxyapatite Based Ceramic from Eggshells: Synthesis and Characterization. Waste and Biomass Valorization, *9*(8), (2018) 1469-1473.https://doi.org/10.1007/s12649-017-9891-3

[19] P. Kamalanathan, S. Ramesh, L.T. Bang, A. Niakan, C.Y. Tan,J. Purbolaksono, H. Chandran, W.D. Teng. Ceramaric International. 40(10) PartB, (2014)16349–16359. https://doi.org/10.1016/j.ceramint.2014.07.074

[20] L. Ćurković, I. Žmak, S. Kurajica, M. Tonković, Z. Šokčević, M.M. Renjo, from Eggshells Biowaste to Hydroxyapatite Biomaterial. Materialwissenschaft Und Werkstofftechnik, 48(8), (2017) 797–802. https://doi.org/10.1002/mawe.20170 0052

[21] S. Pal, A.R. Paul, V.K. Choudhury, M. Balla, A. Das, A. Sinha, Synthesis of Hydroxyapatite from Lates Calcarifer fish Bone for Biomedical Applications. Material Letter, 203, (2017), 89–92. https://doi.org/10.1016/j.matlet.2017.05.103

[22] N. Skandalis, A. Dimopoulou, A. Georgopoulou, N. Gallios, D. Papadopoulos, D. Tsipas , I. Theologidis , N. Michailidis, M. Chatzinikolaidou, The Effect of Silver Nanoparticles Size, Produced Using Plant Extract from Arbutus Unedo, on Their Antibacterial Efficacy Nanomaterials, 7(7), (2017) 178. https://doi.org/10.3390/nano7070178

[23] A.S. Morris, R. Langari, Chapter 3 - Measurement Uncertainty. In Measurement and Instrumentation; Eds.; Butterworth-Heinemann: Boston, MA, USA, (2012) 39–102. https://doi.org/10.1016/B978-0-12-381960-4.00003-6

[24] N. Suwannasingha, A. Kantavong, S. Tunkijjanukij, C. Aenglong, C, H.B. Liu, W. Klaypradit, Effect of Calcination Temperature on Structure and Characteristics of Calcium Oxide Powder Derived from Marine Shell Waste. Journal of Saudi Chemical Society, 26(2), (2022), 101441. https://doi.org/10.1016/j.jscs.2022.101441

[25] M.E.S.I. Saraya, H.H.A.E.L. Rokbaa, Formation and Stabilization of Vaterite Calcium Carbonate by Using Natural Polysaccharide. Advances in Nanoparticles, 06(04), (2017) 158–182. https://doi.org/10.4236/anp.2017.64014

[26] T. Mosmann, Rapid Colorimetric Assay for Cellular Growth and Survival: Application to Proliferation and Cytotoxicity Assays. Journal of Immunological Methods. 65(1-2), (1983) 55-63. https://doi.org/10.1016/0022-1759(83)90303-4

[27] N. Cozza, F. Monte, W. Bonani, P. Aswath, A. Motta, C. Migliaresi, Bioactivity and mineralization of Natural Hydroxyapatite from Cuttlefish Bone and Bioglass. Journal of Tissue Engineering Regeneration Medicine, 12(2), (2018)e1131–e1142. https://doi.org/10.1002/term.2448

[28] A.I. Hussein, Z. Ab-Ghani, A.N.C. Mat, N.A.A. Ghani, A. Husein, I.A. Rahman, Synthesis and Characterization of Spherical Calcium Carbonate Nanoparticles Derived from Cockle Shells. Applied Sciences (Switzerland), 10(20), (2020)7170. https://doi.org/10.3390/app10207170

[29] S.C. Wu, H.K. Tsou, H.C. Hsu, S.K. Hsu, S.P. Liou, W.F. Ho, A Hydrothermal Synthesis of Eggshell and Fruit Waste extract to produce Nanosized Hydroxyapatite. Ceramics International, *39*(7), (2013) 8183-8188. https://doi.org/10.1016/j.ceramint.2013.03.094

[30] G.A. Stanciu, I. Sandulescu, B. Savu, S.G. Stanciu, K.M. Paraskevopoulos, X. Chatzistavrou, E. Kontonasaki, P. Koidis, Investigation of the Hydroxyapatite Growth on Bioactive Glass Surface. Journal of Biomedical and Pharmaceutical Engineering, 1(1), (2007), 34-39.

[31] K. Parajuli, K.P. Malla, N. Panchen, G.C. Ganga, R. Adhikari, Isolation of Antibacterial Nano-Hydroxyapatite Biomaterial from Waste Buffalo Bone and its Characterization. Chemical Technology. 16(1), (2022) 133–141. https://doi.org/10.23939/chcht16.01.133

[32] B.S. Purwasasmita, R. Gultom, Sintesis dan Karakterisasi Serbuk Hidroksiapatit Skala Sub Mikron Menggunakan Metode Presipitasi. *Bionatura*, 10(2), (2008) 155–167.

[33] P. Hui, S.L. Meena, G. Singh, R.D. Agrawal, S. Prakash, Synthesis of Hydroxyapatite Bio-Ceramic Powder by Hydrothermal Method. Journal of Minerals & Materials Characterization & Engineering, 9(8), (2010) 683-692.

[34] T. Dedourkova, J. Zelenka, M. Zelenkova, L. Bene, L. Svoboda, Synthesis of sphere-like nanoparticles of hydroxyapatite. Procedia Engineering, 42, (2012) 816–1821. https://doi.org/10.1016/j.proeng.2012.07.576

[35] M. Boutinguiza, J. Pou, R. Comesaña, F. Lusquiños, A. de Carlos, B. León, Biological hydroxyapatite obtained from fish bones. Materials Science and Engineering C.32 (3), (2012)478–486. https://doi.org/10.1016/j.msec.2011.11.021

[36] M. Markovic, Preparation and Comprehensive Characterization of a Calcium Hydroxyapatite Reference Material Volume. Journal of Research of the National Institute of Standards and Technology, 109, (2004) 553-568.

[37] A.C.S. Jensen, A. Brif, B. Pokroy, M. Hinge, H. Birkedal, Morphology-preserving transformation of minerals mediated by a temperature-responsive polymer membrane: calcite to hydroxyapatite. Crystalline Engineering Communication, 18(13), (2016).2289-2293. https://doi.org/10.1039/C5CE02245B

Authors Contribution Statement

Both the authors equally contributed and approved the final version of this work.

Funding

The authors declare that no funds, grants or any other support were received during the preparation of this manuscript.

Competing Interests

The authors declare that there are no conflicts of interest regarding the publication of this manuscript.

Data Availability

The data supporting the findings of this study can be obtained from the corresponding author upon reasonable request.

Has this article screened for similarity?

Yes

About the License